

# Dynamic Performance Prediction of an Axial Flux Resolver

**Abstract.** The robustness against static eccentricity has caused axial flux resolvers (AFRs) to be proposed in high performance motion control systems. In this paper, the dynamic performance of AFR is predicted using a mathematical model based on d-q axis theory. In particular, the proposed model takes into account the stator currents of brushless AFR and it will be able to model the effect of static eccentricity. Furthermore, it is used to compute the dynamic and steady state equivalent circuits. Finally, the studied AFR is fabricated and tested. Good agreement between simulation results and experimental ones confirms the proposed model.

**Streszczenie.** Analizowano resolver z osiowym strumieniem AFR. Na podstawie modelu matematycznego oceniono właściwości dynamiczne. Szczególną uwagę zwrócono na prąd stojana i efekt ekscentryczności. Przedstawiono układ zastępczy. Zbadano model. (Właściwości dynamiczne resolvera z osiowym strumieniem)

**Keywords:** Axial Flux Brushless Resolver, Dynamic Model, Steady State Performance, Electrical Equivalent Circuit.

**Słowa kluczowe:** resolver, właściwości dynamiczne, obwód zastępczy.

## Introduction

Brushless resolvers have many advantages in comparison with other position sensors. They are more mechanically reliable, and can be easily integrated with motor systems [1]. Furthermore, they have robust structure, wide range of operation temperature, and the ability to reject the common mode noise [2-3]. Beside these advantages the machines with axial flux structure have another major preference. The influence of static eccentricity which is an inevitable error in the bearings of the rotary machines is reduced in axial flux structure [4-5].

Fig. 1 shows the structure of axial flux resolver consisting of an axial flux rotary transformer. The axial flux rotary transformer has a primary winding on the stator and a secondary one on the rotor and it is employed to transfer the exciting signal to the rotating part [6-8].

There are two different methods for modelling and simulating of electrical machines [6-7]:

1) Solving the Maxwell equations on machine geometry by using numerical methods such as two or three dimensional finite element ones (2D or 3D FEM).

2) Solving the flux linkage-current and voltage-current equations by using matlab-simulink.

First method was used in [9] to investigate the effect of skewed rotor and eccentricity error on the accuracy of a conventional brushless resolver by using 2-D finite element analysis. But, the authors of [9] have expressed that there is significant difference between measured and calculated results. Finally, they have justified that their model is not accurate enough.

Although, FEM is an accurate technique for performance prediction of electromagnetic devices, it is very time consuming. In axial flux resolvers the conductors are radially arranged, and thereby the pole pitch and the tooth width will increase when increasing the core diameter. Therefore, the magnetic field distribution of AFRs is non-uniform in the volume of the axial flux resolver. So, a three dimensional (3D) field calculation requiring high amount of memory and high CPU clock frequency is needed [10-11].

The solution is using second method. In this method, it is necessary to solve the differential equation of flux linkage-current and voltage-current. Ref. [12] has presented the simplified form of these equations for radial field (conventional) resolvers. In this research, the stator currents were assumed to be zero and the influence of static eccentricity was ignored. Moreover, the steady state performance of resolver has not been regarded.

Although, the authors of Ref. [13] have taken into account the influence of resolver stator current and eccentricity, they have worked on conventional resolver and they have not derived stator and rotor inductances.

The main objective of this paper is to present a mathematical model based on d-q axis theory to predict the dynamic and static behavior of an axial flux brushless resolver considering eccentricity and stator currents. Dynamic and static equivalent circuit of AFR is derived based on proposed model and the inductances of stator and rotor are expressed regarding geometrical dimensions of AFR. Not only the proposed approach is simple, but also it is accurate and time saving.

Finally, the studied AFR was fabricated and tested with devised test setup. Then simulation results were compared with experimental ones and good agreement of them shows the model ability.

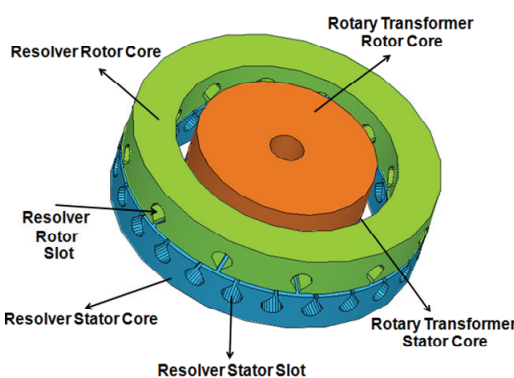


Fig.1. The structure of axial flux resolver

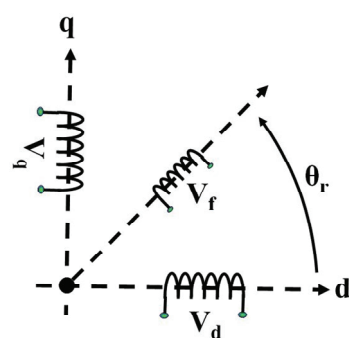


Fig.2. Axial flux resolver windings model

## Axial Flux Resolver Model

The proposed model is based on d-q axis theory. The following assumptions are considered in the analysis [13]:

- a) Stator has two-layer distributed lap windings.
- b) Rotor has a winding with sinusoidal supply.
- c) The inductances of AFR in d-q axis are unequal.

Fig. 2 shows the model of resolver windings. Each stator winding flux consists of leakage flux and main flux, the latter flux links the rotor [14].

### A. Dynamic Model

The voltage equations in machine variables can be expressed as following:

(1)

$$V_r = r_s i_r + L_{rr} \frac{di_r}{dt} + \omega_r L_{sr} \cos \theta_r i_{as} + L_{sr} \sin \theta_r \frac{di_{as}}{dt} + \omega L_{sr} \sin \theta_r i_{bs} - L_{sr} \cos \theta_r \frac{di_{bs}}{dt}$$

(2)

$$\begin{aligned} V_{as} = & -r_s i_{as} + 2\omega_r L_{ms} \sin 2\theta_r i_{as} + L_{ms} \sin 2\theta_r \frac{di_{as}}{dt} \\ & - 2\omega_r L_{ms} \cos 2\theta_r i_{bs} - L_{sr} \sin \theta_r \frac{di_r}{dt} \\ & + \omega_r L_{sr} \cos \theta_r i_r + (\overbrace{L_{ls} + L_0 - L_{ms} \cos 2\theta_r}^{L_s}) \frac{di_{as}}{dt} \end{aligned}$$

(3)

$$\begin{aligned} V_{bs} = & -r_s i_{bs} - 2\omega_r L_{ms} \cos 2\theta_r i_{as} - L_{ms} \sin 2\theta_r \frac{di_{as}}{dt} \\ & - 2\omega_r L_{ms} \sin 2\theta_r i_{bs} + \omega_r L_{sr} \sin \theta_r i_r \\ & + (\overbrace{L_{ls} + L_0 + L_{ms} \cos 2\theta_r}^{L'_s}) \frac{di_{bs}}{dt} - L_{sr} \cos \theta_r \frac{di_r}{dt} \end{aligned}$$

In the above equations the *s* and *r* subscripts denote variables and parameters associated with the stator and rotor circuits, respectively.  $V_{as}$ ,  $V_{bs}$  are the stator voltages,  $V_r$  is the excitation signal of the resolver ( $V_r = v_r \cos(\omega_r t + \psi)$ ),  $i_{as}$ ,  $i_{bs}$  are the stator currents,  $i_r$  is the rotor current,  $r_s$  is the resistance of stator circuit,  $L_{ls}$ ,  $L_{ms}$  are the leakage and magnetizing inductances of the stator winding, respectively,  $r_r$ ,  $L_{rr}$  are the resistance and self inductance of rotor circuit,  $L_{sr}$  is the mutual inductance between the rotor and stator circuits,  $\omega_r$  is the rotor angular velocity and  $\theta_r$  is electrical angular displacement. The inductances of AFR can be calculated as [15-16]:

$$(4) \quad L_{ls} = \frac{1}{2Pq} N_s^2 (R_0 - R_i) (\lambda_s + \lambda_o + \lambda_d + \lambda_z) \times 10^{-5}$$

$$(5) \quad L_{lr} = \frac{1}{2Pq} N_r^2 (R_0 - R_i) (\lambda_s + \lambda_o + \lambda_d + \lambda_z) \times 10^{-5}$$

$$(6) \quad L_{ms} = \frac{\mu_0 \pi (R_o^2 - R_i^2) N_s^2}{8P^2 g}$$

$$(7) \quad L_{rr} = \frac{\mu_0 \pi (R_o^2 - R_i^2) N_r^2}{8P^2 g} + L_{lr}$$

$$(8) \quad L_{sr} = \frac{\mu_0 \pi (R_o^2 - R_i^2) N_s N_r}{8P^2 g}$$

Where  $P$  is the pole pair number,  $q$  is the number of slots per pole per phase,  $R_o$  and  $R_i$  are outer and inner radius of core,  $\lambda_s$  is specific slot leakage permeance,  $\lambda_o$  is specific overhang leakage permeance,  $\lambda_d$  is specific differential leakage permeance,  $\lambda_z$  is specific zig-zag

leakage permeance,  $g$  is effective air-gap length between the surface of stator and rotor,  $N_s$  and  $N_r$  are the number of stator and rotor turns, respectively in each phase.

The stator variables are transferred to the rotor reference frame which eliminates the time-varying inductances in the voltage equations. Park's equations are obtained by setting the speed of the stator frame equal to the rotor speed.

The expressions for the flux linkages are:

(9)

$$\lambda_q = (L_{ls} + L_0 - L_{ms}) i_q = (L_{ls} + L_{mq}) i_q$$

$$\lambda_d = (L_{ls} + L_0 + L_{ms}) i_d + L_{md} i_r = (L_{ls} + L_{md}) i_d + L_{md} i_r$$

$$\lambda_r = L_{md} i_d + (L_{lr} + L_{md}) i_r$$

And

$$(10) \quad \psi = \omega_b \lambda$$

$$x = \omega_b L$$

Then

$$\psi_q = (X_{ls} + X_{mq}) i_q = X_{ls} i_q + \psi_{mq}$$

$$(11) \quad \psi_d = (X_{ls} + X_{md}) i_d + X_{md} i_r = X_{ls} i_d + \psi_{md}$$

$$\psi_r = X_{md} i_d + (X_{lr} + X_{md}) i_r = X_{lr} i_r + \psi_{md}$$

By referring rotor variables to the stator windings, voltage equations can be written as:

$$V_q = -r_s i_{qs} + \frac{1}{\omega_b} \frac{d\psi_q}{dt} + \frac{\omega_r}{\omega_b} \psi_d$$

$$(12) \quad V_d = -r_s i_{ds} + \frac{1}{\omega_b} \frac{d\psi_d}{dt} - \frac{\omega_r}{\omega_b} \psi_q$$

$$V'_r = r'_r i'_r + \frac{1}{\omega_b} \frac{d\psi_r}{dt}$$

In order to obtain the equivalent circuits, equation (12) should be replaced by equation (11). Thus, the voltage-current equations are as following:

$$(13) \quad \begin{bmatrix} V_q \\ V_d \\ V'_r \end{bmatrix} = \begin{bmatrix} -r_s + \frac{p}{\omega_b} X_q & \frac{\omega_r}{\omega_b} X_d & \frac{\omega_r}{\omega_b} X_{md} \\ -\frac{\omega_r}{\omega_b} X_q & -r_s + \frac{p}{\omega_b} X_d & \frac{p}{\omega_b} X_{md} \\ 0 & \frac{p}{\omega_b} X_{md} & r'_r + \frac{p}{\omega_b} X'_{rr} \end{bmatrix} \times \begin{bmatrix} i_q \\ i_d \\ i'_r \end{bmatrix}$$

Where:

$$(14) \quad X_q = X_{ls} + X_{mq}, X_{mq} = X_0 - X_{ms}$$

$$X_d = X_{ls} + X_{md}, X_{md} = X_0 + X_{ms}$$

And  $p$  is  $d/dt$  [14].

The electrical equivalent circuits of the resolver are presented in Fig. 3.

The electromagnetic torque developed in the resolver is given by:

$$(15) \quad T_{em} = \frac{P}{2\omega_b} (\psi_d i_q - \psi_q i_d)$$

And the mechanical equation of resolver in per unit can be written as:

$$(16) \quad T_{mech}(pu) - T_{em}(pu) - T_{damp}(pu) = 2H \frac{d(\omega_r / \omega_b)}{dt}$$

Where  $H$  is inertia constant expressed in second,  $T_{mech}$  is load torque and  $T_{damp}$  is frictional torque.

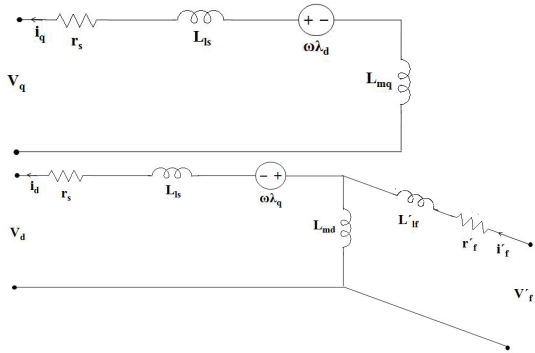


Fig.3. Dynamic electrical equivalent circuits of the AFR in d-q axis

### B. Steady State Model

In steady state, the electrical angular velocity of the rotor is constant and equal to  $\omega_e$ . In this mode of operation the rotor windings do not experience any change of flux linkages [17]. Thus, with  $\omega_r$  equal to  $\omega_e$  and the time rate of change of all flux linkages neglected, the steady state versions of (9) and (10) become:

$$(17) \quad V_q^e = V_q = -r_s I_q - \frac{\omega_e}{\omega_b} x_d I_d + \frac{\omega_e}{\omega_b} x_{md} I'_r$$

$$V_d^e = V_d = -r_s I_d + \frac{\omega_e}{\omega_b} x_q I_q$$

$$V_r'^e = V_r' = -r'_r I'_r$$

Here the  $\omega_e$  to  $\omega_b$  ratio is again included to accommodate analysis when the operation frequency is other than rated. In the synchronously rotating reference frame and using uppercase letters to denote the constant steady state variables [17]:

$$(18) \quad \sqrt{2} \tilde{F}_{as} = F_{qs}^e - j F_{ds}^e$$

Where  $F$  is each electrical variable (voltage, current, flux linkage),  $\tilde{F}$  is a phasor which represents a sinusoidal quantity,  $F_{qs}^e$  and  $F_{ds}^e$  are real quantities representing the constant steady state variables of the synchronously rotating reference frame. Hence:

$$(19) \quad \sqrt{2} \tilde{V}_{as} = V_q^e - j V_d^e$$

Substituting (17) into (19) yields:

$$(20) \quad \sqrt{2} \tilde{V}_{as} = \left[ r_s + \frac{\omega_e}{\omega_b} X_q \right] \tilde{I}_d + \frac{1}{\sqrt{2}} \left[ -\frac{\omega_e}{\omega_b} (X_d - X_q) I_d + \frac{\omega_e}{\omega_b} X_{md} I'_r \right]$$

For symmetrical resolver,  $X_d = X_q$  and  $\omega_e = \omega_b$ . So (20) can be rewritten as:

$$(21) \quad \tilde{V}_{as} = -(r_s + j X_s) \tilde{I}_{as} + \tilde{E}_a$$

$$\tilde{E}_a = \frac{1}{\sqrt{2}} X_m I'_r$$

where

$$(22) \quad X_s = X_{ls} + X_m$$

Considering above equations, the steady state equivalent circuit of resolver is shown in fig. 4.

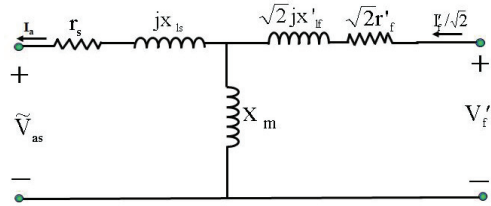


Fig.4. Steady state equivalent circuit of the AFR

### Simulation

The state equations on the rotating d-q reference frame are introduced. MATLAB/Simulink software is used for simulation.

Input, output, and state variables are:

State Variables =  $[\Psi_{qs}, \Psi_{ds}, \Psi'_r]$

Input Vector =  $[V_r', \Delta T_{mech}]$

Output Vector =  $[\Delta \theta_r]$

In generalized theory of electrical machines, it is more convenient to use flux linkages as the state variables [17-18]. By this way, the differential operators change to integral operators. Using Equation (11) and (13), the flux-linkages equations could be obtained as follow:

$$(23) \quad \psi_q = \omega_b \int \left( V_q + \frac{r_s}{X_{ls}} (-\psi_{mq} + \psi_q) - \frac{\omega_r}{\omega_b} \psi_d \right) dt$$

$$(24) \quad \psi_d = \omega_b \int \left( V_d + \frac{r_s}{X_{ls}} (-\psi_{md} + \psi_d) + \frac{\omega_r}{\omega_b} \psi_q \right) dt$$

$$(25) \quad \psi'_r = \omega_b \int \left( V_r' + \frac{r'_r}{X'_{lr}} (\psi_{md} - \psi'_r) \right) dt$$

Where

$$(26) \quad \psi_{md} = \left( \frac{1}{X_{md}} + \frac{1}{X'_{lr}} + \frac{1}{X_{ls}} \right)^{-1} \left( \frac{\psi_d}{X_{ls}} + \frac{\psi'_r}{X'_{lr}} \right)$$

$$(27) \quad \psi_{mq} = \left( \frac{1}{X_{mq}} + \frac{1}{X_{ls}} \right)^{-1} \frac{\psi_q}{X_{ls}}$$

And angular position, stator, and rotor currents can be calculated as:

$$\theta(t) = \delta(t) = \theta_r(t) - \theta_e(t)$$

$$(28) \quad = \int_0^t (\omega_r - \omega_e) dt + \theta_r(0) - \theta_e(0)$$

$$(29) \quad i_q = \frac{\psi_q - \psi_{mq}}{X_{ls}}$$

$$(30) \quad i_d = \frac{\psi_d - \psi_{md}}{X_{ls}}$$

$$(31) \quad i'_r = \frac{\psi'_r - \psi_{md}}{X'_{lr}}$$

Because of the ability of proposed model to assume different values for  $L_d$  and  $L_q$ , it can consider the effect of eccentricity in AFR which is investigated in our outgoing paper.

Fig. 5 shows a block diagram which is used in simulation.

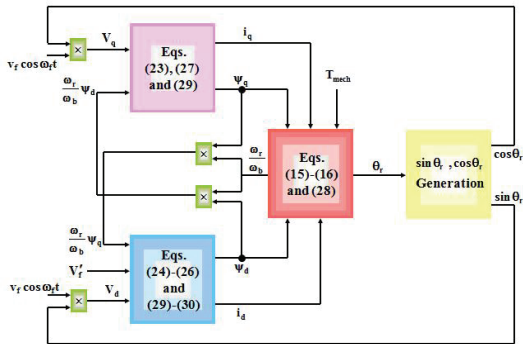


Fig.5. Block diagram of AFR simulation

## Results and Discussions

Fig. 6 shows the stator and rotor of fabricated AFR before and after winding. This prototype has single stator and single rotor structure.

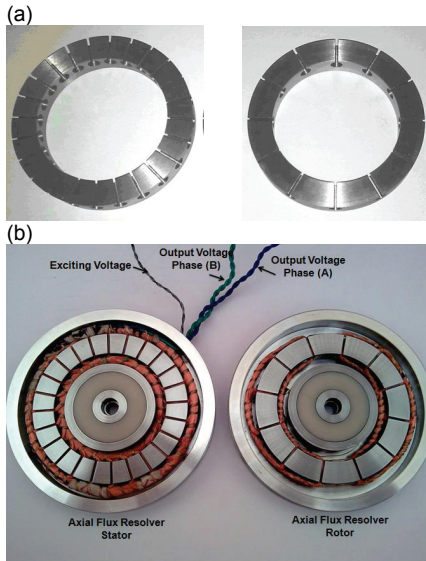


Fig.6 The stator and rotor of manufactured resolver, (a) before winding, and (b) after winding

The specifications of this AFR are presented in Table I and the parameters of its equivalent circuit are given in Table II. These parameters are obtained using DC-Pulse method [14]. In this method stator winding is charged with its nominal DC current. The current signal is shown in Fig. 7 (with 1 mm air gap length).

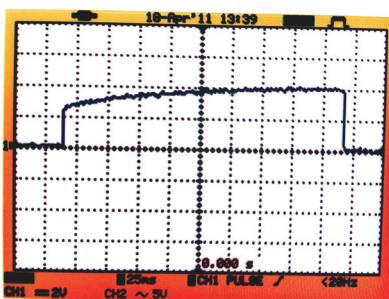


Fig.7. charge current of stator winding

The literature regarding the resolver reported previously, usually have discuss about position error distribution. Since the position signal is resulted from the ratio of d-q voltages, in this paper these voltages are reported, too. On the other hand, the input resistance of resolver to digital converter (RDC) is very high. Therefore, the current in the stator coils of AFR, which apply to the RDC, is in the order of micro

ampere [19]. According to this conditions, Fig. 8 shows the simulated and measured voltages of axial flux resolver with the nominal excitation frequency (4 kHz) and 60  $\mu$ A stator output currents (5 times of the RDC nominal input current).

Table 1. The Specifications of Tested Axial Flux Resolver

Parameter	Unit	Value
Frequency	Hz	4000
Peak to Peak input voltage	V	10
Maximum position error	Arcmin	10
Pole number	-	2
Maximum speed	rpm	8000-12000
Air gap length	mm	1
Core outer /inner diameters	mm	72/52
Core length, stator/rotor	mm	10/10
Duty cycle	-	S <sub>1</sub>
Number of turns, Stator/Rotor	-	1200/600

Table 2. The Equivalent Circuit Parameters of Tested AFR

Parameter	Unit	Value
r <sub>s</sub>	$\Omega$	290
r' <sub>f</sub>	$\Omega$	17
L <sub>m</sub>	H	$3.41 \times 10^{-3}$
L' <sub>if</sub>	H	$0.11 \times 10^{-3}$
L <sub>ls</sub>	H	$0.11 \times 10^{-3}$
J	$\text{kg} \cdot \text{m}^2$	$9.13 \times 10^{-4}$

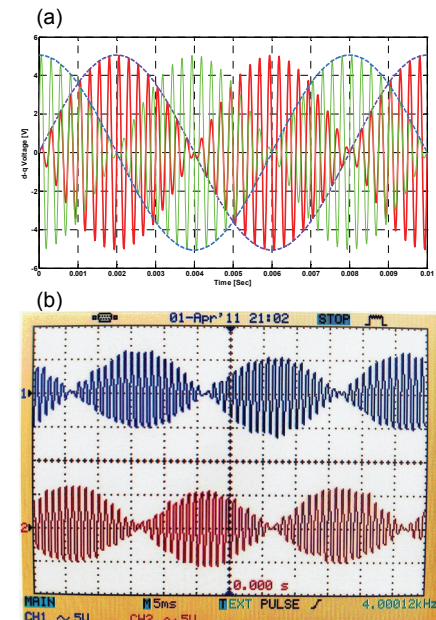


Fig.8. Output voltage of resolver versus time with 4 kHz excitation and 60  $\mu$ A output currents, (a) simulated d-q- voltages, (b) measured q-d voltages.

Table III shows the comparison of simulated and experimental output voltages. Results show good agreement between test and simulation voltages (about 2.88% error).

Table 3. The comparisons of calculated and measured results

Output current (mA)	Frequency (Hz)	Output voltage (simulated)	Output voltage (measured)	Error (%)
0.060	4000	5.06	5.21	2.88

To study on AFR as a position sensor, a test setup must be constructed. So, a rotary test bed was devised and a precision rotary tycope was placed on it. Fig. 9 shows view of this setup. So, a rotary test bed was provided and a precision rotary tycope was placed on it. Different rotary positions are produced by this tycope in  $[0, 2\pi]$  rad.

Resolver output and simulation results are compared in each of these positions (The resolver output is obtained from arctangent of output voltages ratio).

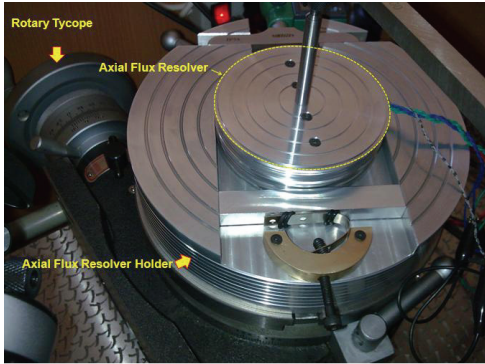


Fig.9. View of the test setup of AFR as a position sensor

Fig. 10 shows the comparison of simulated and measured output position of AFR and their difference. This figure shows the maximum position error difference between measured and simulated results is 6 Arcmin at 245 degree. But, the maximum position error of simulated and fabricated AFR versus real position are about 9 and 5 Arcmin at  $300^\circ$  and  $325^\circ$  respectively.

In proposed model, d-q axis inductances are different parametric variables. By using unequal values for  $L_d$  and  $L_q$  eccentricity of resolver can be modeled. We have studied a new method based on this model for eccentricity detection and its effect restriction that will be published in outcoming papers.

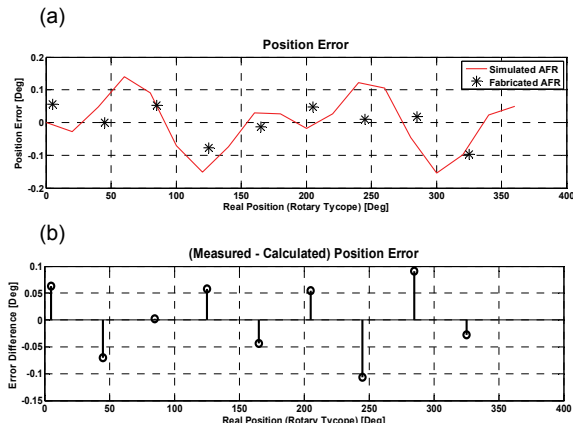


Fig.10. Comparison of calculated angular position with resolver output versus reference position (generated by rotary tycope) (a) position error, and (b) error difference between measured and calculated data

## Conclusions

An axial flux brushless resolver (AFR) was analyzed. Its dynamic and steady state equivalent circuits were presented. Moreover, the stator currents were taken into account in the proposed model. In studied d-q model  $L_d$  and  $L_q$  were assumed differently. So, proposed model will be able to consider the effect of eccentricity which will be reported in next papers. Studied AFR and its test setup were manufactured and its parameters were measured using DC-Pulse method. These parameters were used to simulate the d-q model of AFR. Output signals of AFR were monitored by a 1 Giga-sample per second (1GS/s) digital oscilloscope. Then, comparison between experimental and simulation results shows the error of 2.88% in output voltages amplitude. Using test setup resulted that the maximum position error difference between measured and simulated results is 6 Arcmin. But, the maximum position

error of simulated and fabricated AFR versus real position are about 9 and 5 Arcmin, respectively. These results demonstrate the accuracy of the proposed model for AFR.

## REFERENCES

- [1] L. Sun, "Analysis and improvement on the Structure of variable reluctance resolver", *IEEE Trans. on Magn.*, 44 (Aug. 2002), no. 8, pp. 2002-2008.
- [2] M. Benamar, L. Ben-brahim, M. A. Alhamadi, M. Al-Naemi, "A novel method for estimating the angle from analog co-sinusoidal quadrature signals", *Sensors and Actuators (Elsevier B.V.)*, vol. 142, pp. 225–231, 2008.
- [3] M. L. Mingji, Y. Yu, Z. Jibin, L. Yongping, N. Livingstone and G. Wenxue, "A high Error analysis and compensation of multipole resolvers", *Meas. Sci. Technol.* 10 (1999), pp. 1292–1295.
- [4] X. Li, Q. Wu, and S. Nandi, Performance Analysis of a Three-Phase Induction Machine with Inclined Static Eccentricity", *IEEE Trans. on Industry Applications*, 43 (March/April 2007), no. 2, pp. 531-541.
- [5] D.G. Dorrell, W.T. Thomson, and S. Roach, Analysis of Air-Gap Flux, Current, Vibration Signals as a Function of the Combination of Static and Dynamic Air-Gap Eccentricity in 3-Phase Induction Motors, *IEEE Trans. on Industry Applications*, 33 (Jan./Feb. 1997), no. 1, pp. 24–34.
- [6] A. Bünt, S. Beinek, High-Performance Speed Measurement by Suppression of Systematic Resolver and Encoder Errors , *IEEE Trans. on Industrial Electronics*, 51 (Feb. 2004), no. 1, pp. 49-53.
- [7] Y. Huang, Ch. Chen and W. Shu, Finite Element Analysis on Characteristics of Rotary Transformers , *IEEE Trans. on Magn.*, 30 (Nov. 1994), no. 6, pp. 4866-4868.
- [8] H. Inoue, H. Fusayasu and N. Takahari, Investigation of Factors Affecting Crosstalk in a Rotary Transformer , *IEEE Trans. on Magn.*, 33 (March 1997), no 2, pp. 2215-2218.
- [9] K. Masaki, K. Kitazawa, H. Mimura, M. Nirei, K. Tsuchimichi, H. Wakiwaka and H. Yamada, Magnetic Field Analysis of a Resolver with a Skewed and Eccentric Rotor , *Elsevier Trans. On Sensors and Actuators*, 81 (April 2000), pp. 297-300.
- [10] M. Valtonen, Performance Characteristics of an Axial-Flux Solid-Rotor-Core Induction Motor , *Phd thesis, Lappeenranta University of Technology*, Lappeenranta, Finland, 2007.
- [11] M. Lukanszyn, M. Jagieła, R. Wrobel, A Disc Type Motor with Co-axial Flux in the Stator Influence of Magnetic Circuit Parameters on the Torque , *Springer-Verlag, Electrical Engineering*, 84 (may 2002), no. 2, pp. 91-100.
- [12] W. Jiuqing, L. Xingshan and G. Hong, The Analysis and Design of High-Speed Brushless Resolver Plus R/D Converter Shaft-Angle Measurement System , *Electrical Machines and Systems International Conf. (ICEMS 2001) Proc.*, Shenyang, China, 2001, 1, pp. 289 - 292.
- [13] D. A. Khaburi, F. Tootoonchian and Z. Nasiri-Gheidari, Dynamic Performance Prediction of Brushless Resolver , *Iranian Journal of Electrical & Electronic Engineering*, 4 (July 2008), no. 3, pp. 94-103.
- [14] D.A. Khaburi, F. Tootoonchian, Z. Nasiri-Gheidari, Parameter Identification of a Brushless Resolver Using Charge Response of Stator Current , *Iranian Journal of Electrical & Electronic Engineering*, 3 (Jan. 2007), no. 1&2, pp. 42-52.
- [15] C.C. Chan, Axial-Field Electrical Machines Design and Applications , *IEEE Tran. on Energy Conversion*, EC-2 (June 1987), no. 2, pp. 294-300.
- [16] C. Zhange, K.J. Tseng and T.D. Nguyen, Analysis and Comparison of Axial Flux PM Synchronous Motor and Induction Motor , *9th IEEE International Power & Energy Conf. (IPEC 2010) Proc.*, Suntec, Singapore, 27 - 29 Oct. 2010, 1, pp. 572-577.
- [17] P.C. Krause, Analysis of Electrical Machinery , *McGraw-Hill series in electrical engineering, Power & energy*, 1986.
- [18] C.M. Ong, Dynamic Simulation of Electric Machinery Using Matlab/Simulink , *Prentice Hall PTR. Upper Saddle River, New Jersey*, 1998.
- [19] Analog Device Company, RDC Datasheets , presented at <http://www.analog.com>, received at 10 Nov. 2010.

**Authors:** Corresponding author: Farid Tootoonchian, Ph.D. Candidate of Electrical and Computer Engineering, K. N. Toosi University of Technology, Tehran, Iran, E-mail: [Tootoonchian@iust.ac.ir](mailto:Tootoonchian@iust.ac.ir), Dr. M. Ardebili, and Dr. K. Abbaszadeh who are the Faculty of Electrical and Computer Engineering, K. N. Toosi University of Technology, Tehran, Iran. And their E-mail addresses are [Ardebili@kntu.ac.ir](mailto:Ardebili@kntu.ac.ir), and [Abbaszadeh@kntu.ac.ir](mailto:Abbaszadeh@kntu.ac.ir) respectively.